

Efficacy of Dual Inhibition of Glycolysis and Glutaminolysis for Therapy of Renal Lesions in *Tsc2*^{+/-} Mice¹



Ashley T. Jones, Kalin Narov, Jian Yang, Julian R. Sampson and Ming Hong Shen

Institute of Medical Genetics, Division of Cancer and Genetics, School of Medicine, Cardiff University, Heath Park, Cardiff CF14 4XN, UK

Abstract

Tuberous sclerosis is caused by mutations in the *TSC1* or *TSC2* gene and characterized by development of tumors in multiple organs including the kidneys. TSC-associated tumors exhibit somatic loss of the second allele of the TSC genes, leading to aberrant activation of the mechanistic target of rapamycin (mTOR) signaling pathway. Activation of mTOR complex 1 (mTORC1) causes addiction to glucose and glutamine in *Tsc1*^{-/-} or *Tsc2*^{-/-} mouse embryonic fibroblasts (MEFs). Blocking of glutamine anaplerosis in combination with glycolytic inhibition causes significant cell death in *Tsc2*^{-/-} but not *Tsc2*^{+/+} MEFs. In this study, we tested efficacy of dual inhibition of glycolysis with 3-BrPA and glutaminolysis with CB-839 for renal tumors in *Tsc2*^{+/-} mice. Following 2 months of treatment of *Tsc2*^{+/-} mice from the age of 12 months, combination of 3-BrPA and CB-839 significantly reduced overall size and cellular areas of all renal lesions (cystic/papillary adenomas and solid carcinomas), but neither alone did. Combination of 3-BrPA and CB-839 inhibited mTORC1 and the proliferation of tumor cells but did not increase apoptosis. However, combination of 3-BrPA and CB-839 was not as efficacious as rapamycin alone or rapamycin in combination with either 3-BrPA or CB-839 for renal lesions of *Tsc2*^{+/-} mice. Consistently, rapamycin alone or rapamycin in combination with either 3-BrPA or CB-839 had stronger inhibitory effects on mTORC1 and proliferation of tumor cells than combination of 3-BrPA and CB-839. We conclude that combination of 3-BrPA and CB-839 may not offer a better therapeutic strategy than rapamycin for TSC-associated tumors.

Neoplasia (2019) 21, 230–238

Introduction

Tuberous sclerosis is caused by mutations in the *TSC1* or *TSC2* gene and characterized by development of tumors in different organs [1]. Over 80% of TSC patients develop multiple and bilateral angiomyolipomas in the kidneys that are the leading cause of adult deaths from the disease. Around 50% of TSC patients have renal cysts, and approximately 4% of TSC patients suffer from renal carcinomas. The *TSC1/TSC2* complex downregulates the mechanistic target of rapamycin (mTOR) signaling pathway through its GTPase activating protein (GAP) activity towards the small G-protein Rheb (Ras homologue enriched in brain) [2]. TSC-associated tumors exhibit somatic loss of the second allele of the TSC genes, giving rise to aberrant activation of the mTOR signaling pathway in human and mouse [3,4]. Rapamycin and its analogs (rapalogs) are allosteric mTOR inhibitors and reduce size of TSC-associated tumors, but these tumors regrow upon cessation of treatment [5–7]. Activation of mTOR complex 1 (mTORC1) promotes glycolysis and glutaminolysis in *Tsc2*^{-/-} mouse embryonic fibroblasts (MEFs) that are addicted to glucose and

glutamine [8,9]. Glycolytic inhibition suppresses tumor growth in a mouse model transplanted with *Tsc2*^{-/-} rat tumor cells [10]. Blocking of glutamine anaplerosis in combination with glycolytic inhibition causes significant cell death in *Tsc2*^{-/-} but not *Tsc2*^{+/+} MEF cells [9]. Dual inhibition of glycolysis and glutaminolysis may provide a new approach to treating tumors lacking *TSC1* or *TSC2*.

The pyruvate analog 3-bromopyruvate (3-BrPA) is an efficient inhibitor of glycolysis through alkylating glycolytic enzymes,

Address all correspondence to: Ming Hong Shen.

E-mail: shenmh@cf.ac.uk

¹ Financial support: This project was supported by the Wales Gene Park and the Tuberous Sclerosis Association.

Received 25 October 2018; Revised 12 December 2018; Accepted 13 December 2018

© 2018 The Authors. Published by Elsevier Inc. on behalf of Neoplasia Press, Inc. This is an open access article under the CC BY-NC-ND license (<http://creativecommons.org/licenses/by-nc-nd/4.0/>).

1476-5586

<https://doi.org/10.1016/j.neo.2018.12.003>

particularly hexokinase II (HK2) and glyceraldehyde 3-phosphate dehydrogenase (GAPDH) [11]. Being well tolerated, 3-BrPA is very effective for treating liver carcinomas in rabbit and mouse models [12]. CB-839 is a potent blocker of glutaminolysis by selectively inhibiting glutaminase (GLS). Preclinical studies have suggested effective antitumor activity of CB-839 in various types of cancer [13–16].

In this study, we tested efficacy of dual inhibition of glycolysis with 3-BrPA and glutaminolysis with CB-839 for renal tumors in *Tsc2^{+/-}* mice. We found that combination of 3-BrPA and CB-839 significantly reduced overall size and cellular areas of all renal lesions including cystic/papillary adenomas and solid carcinomas, but neither alone did. However, combination of 3-BrPA and CB-839 was not as efficacious as rapamycin alone or rapamycin in combination with either 3-BrPA or CB-839 for renal tumors of *Tsc2^{+/-}* mice.

Materials and Methods

Animal Procedures

Animal procedures were performed in accordance with the UK Home Office guidelines and approved by the Ethical Review Group of Cardiff University. *Tsc2^{+/-}* mice were described previously [17]. To test antitumor efficacy of dual inhibition of glycolysis and glutaminolysis for renal tumors, *Tsc2^{+/-}* balb/c litter mates were randomly allocated into seven groups, balanced for gender and of the same age. *Tsc2^{+/-}* mice were treated for 2 months from the age of 12 months with vehicle (10 μ l/g) ($n = 17$), 3-BrPA (3 mg/kg) ($n = 19$), CB-839 (200 mg/kg) ($n = 20$), rapamycin (4 mg/kg) ($n = 20$), 3-BrPA (3 mg/kg) plus rapamycin (4 mg/kg) ($n = 18$), CB-839 (200 mg/kg) plus rapamycin (4 mg/kg) ($n = 20$), or 3-BrPA (3 mg/kg) plus CB-839 (200 mg/kg) ($n = 18$). Vehicle or CB-839 was administered twice daily *via* gavage, and 3-BrPA or rapamycin was administered 5 times a week *via* intraperitoneal injection. Following treatment, mice were sacrificed for assessment of tumor burden and analysis of protein expression and phosphorylation in the kidneys. Vehicle and CB-839 were supplied by Calithera Biosciences, Inc., South San Francisco, CA. Rapamycin was purchased from LC Laboratories, Woburn, MA, and 3-BrPA was from Sigma-Aldrich, Dorset, UK.

Histology

Assessment of tumor burden in the kidneys of mice was performed as described previously [18]. Mouse kidneys were fixed in 10% buffered formalin saline (Thermo Scientific, Runcorn, UK) for 24 hours. Fixed kidneys were processed and paraffin embedded. Six coronal sections of 5 μ m were prepared at 200- μ m intervals from each kidney. Kidney sections were hematoxylin and eosin (HE)-stained and scanned to create virtual slides using an Aperio system (<http://www.aperio.com/?gclid=CNXN-8by4aUCFcinfaods3eg1w>). Virtual slides were used to quantify lesions for tumor burden estimation. Maximum cross-sectional whole area (lesion size) and cellular area of each renal lesion were measured using ImageJ (<http://rsbweb.nih.gov/ij/>). Cellular areas of renal lesions were obtained from parenchyma and stroma. Tumor burdens for all lesions (cystic/papillary adenomas and solid carcinomas) and solid carcinomas alone were estimated, respectively. Analysis was conducted blindly with respect to treatment status.

Immunohistochemistry (IHC)

Kidney sections prepared as described above were used for IHC. Conventional IHC was performed as described previously [19]. Multiple sequential IHC (MS-IHC) was performed to colocalize multiple antigens in the same cells using the same tissue sections. A

crucial step of MS-IHC was to completely strip previous primary antibodies to ensure efficiency and specificity of subsequent primary antibody-antigen reactions. The protocol used for stripping antibodies was modified from Kim et al. [20]. For MS-IHC, previous IHC-stained slides were incubated in xylene for 10 minutes to remove coverslips and then incubated at 50°C in a buffered solution containing 5% SDS, 0.5% mercaptoethanol, and 50 mM Tris-HCl (pH 7.5) for 60 minutes to strip antibodies, and finally, the protocol was followed for conventional IHC. Primary antibodies against GAPDH, HK2 and glutamate dehydrogenase (GDH), and phosphorylated S6 ribosomal protein at S235/236, 4E-BP1 at T37/46, and Akt at S473 were supplied by Cell Signalling Technology, Danvers, MA; phosphorylated PKC α at S657 by Santa Cruz Biotechnology Inc., Dallas, TX; GLS, Ki67, and active Caspase-3 by Abcam, Cambridge, UK; and MCT1 by Insight Biotechnology, Wembley, UK. SignalStain Boost Rabbit specific IHC Detection Reagent (Cell Signalling Technology, Danvers, MA) and ImmPACT NovaRED Peroxidase (HRP) Substrate (Vector Laboratories Ltd., Peterborough, UK) were used to stain antigens.

Western Blot

For Western analysis, proteins of kidney tissues were prepared from *Tsc2^{+/-}* mice treated as described above using AllPrep DNA/RNA/Protein Mini Kit (QIAGEN Ltd-UK, Crawley, UK). Twenty micrograms of protein per sample was separated on NuPAGE 4%-12% Bis-Tris Gels (Fisher Scientific UK Ltd., Loughborough, UK) and transferred onto Hybond ECL Membranes (GE Healthcare UK Ltd., Little Chalfont, UK). Blots were analyzed with ECL Select Western Detection Kit (GE Healthcare UK Ltd.), and signals were detected using Autochemi Imaging System (UVP, Upland, CA). In addition to primary antibodies described above, primary antibodies against β -actin and phosphorylated Akt at T450 were supplied by Cell Signalling Technology, Danvers, MA; phosphorylated mTOR at S2448 and S2481 by Sigma-Aldrich, Dorset, UK; and PKC α at T638 by Abcam, Cambridge, UK. Horseradish peroxidase-conjugated secondary antibody against rabbit was supplied by Cell Signalling Technology, Danvers, MA.

Statistical Analysis

The Mann-Whitney test was performed to compare tumor burden and proliferation of tumor cells between treatment groups. $P < .05$ was considered to be statistically significant. Analyses were performed using GraphPad Prism 7.03.

Results

Aberrant Activation of mTOR Signaling and Expression of Enzymes Crucial for Glycolysis and Glutaminolysis in Renal Tumors of *Tsc2^{+/-}* Mice

Tsc2^{+/-} mice spontaneously develop renal lesions including cystic/papillary adenomas and solid carcinomas. As reported previously [19], both mTORC1 and mTORC2 were aberrantly activated in renal tumors of *Tsc2^{+/-}* mice as indicated by increased phosphorylation of ribosomal protein S6 at S235/236, 4E-BP1 at T37/46, Akt at S473, and PKC α at S657 (Figure 1). GAPDH and HK2 are important glycolytic enzymes. GLS and GDH are enzymes crucial for glutaminolysis. As shown in Figure 2, GAPDH was highly expressed in papillary adenomas and carcinomas. HK2 was less expressed in papillary adenomas, but its expression was increased in carcinomas (Figure 2). The GLS level was variable in papillary adenomas and

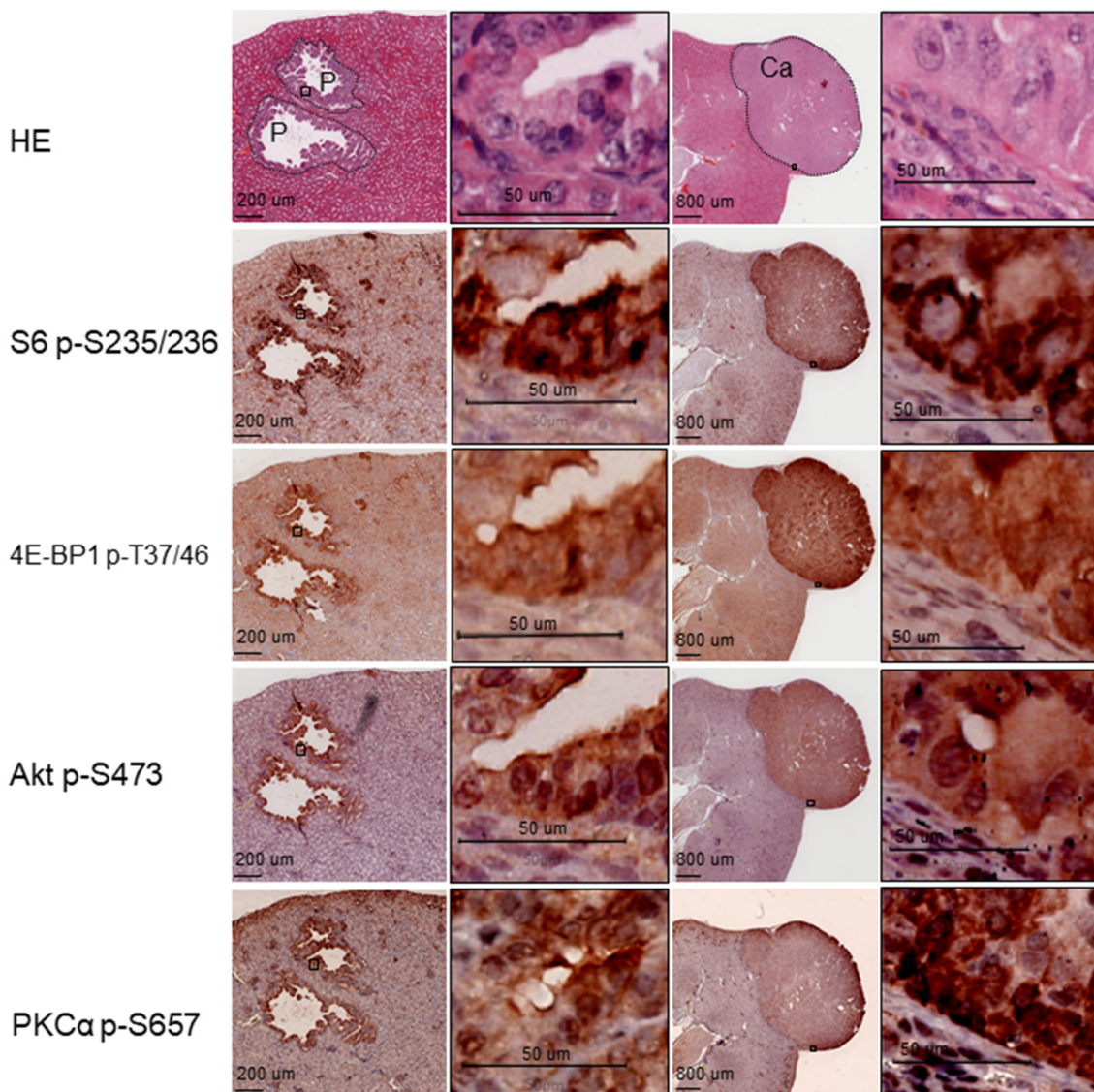


Figure 1. mTOR signaling in renal tumors of *Tsc2*^{+/-} mice. Adjacent kidney sections prepared from 14-month-old *Tsc2*^{+/-} mice were used for HE and IHC or MS-IHC. The same sections were subjected to three rounds of IHC to detect phosphorylation of S6 at S235/236, 4E-BP1 at T37/46, and Akt at S473. Phosphorylation of PKCα at S657 was stained on a separate adjacent section. Representative stained sections were presented to show phosphorylation levels of the corresponding proteins in renal lesions. *P*, papillary adenoma; *Ca*, carcinoma. Black lines are scale bars.

significantly increased in carcinomas (Figure 2). Highly expressed GDH was also observed in papillary adenomas and carcinomas (Figure 2).

*Efficacy of Dual Inhibition of Glycolysis and Glutaminolysis for Therapy of Renal Tumors in *Tsc2*^{+/-} Mice*

We tested efficacy of dual inhibition of glycolysis and glutaminolysis with 3-BrPA and CB-839 for therapy of renal tumors in *Tsc2*^{+/-} mice. 3-BrPA is an efficient inhibitor of GAPDH and HK2, and CB-839 is a potent inhibitor of GLS. We first examined the expression of monocarboxylate transporter 1 (MCT1) since it is required for efficient delivery of 3-BrPA to tumor cells [21]. MCT1 was highly expressed in all tumor cells of renal cystic/papillary adenomas and carcinomas in *Tsc2*^{+/-} mice (Figure 3). We then treated *Tsc2*^{+/-} mice for 2 months from the age of 12 months as summarized in Table 1. Three mice treated with 3-BrPA alone, three with combination of

3-BrPA and rapamycin, and four with combination of 3-BrPA and CB-839 were killed due to significant loss of body weight within the first month of treatment and excluded from further analysis in this study. Tumor burden was compared by analyzing total number, size, and cellular areas of all lesions (cystic/papillary adenomas and solid carcinomas) and solid carcinomas alone, respectively (Figure 4). When all lesions are analyzed, combination of 3-BrPA and CB-839 significantly reduced overall lesion size ($P = .0209$) and cellular area ($P = .0397$) (Figure 4; Supplementary Table 1). Combination of 3-BrPA and CB-839 appeared to reduce total number of all lesions, but the reduction did not reach statistical significance. Rapamycin alone or rapamycin plus 3-BrPA or rapamycin plus CB-839 significantly reduced total number ($P < .0001$, $P < .0001$, $P < .0001$), size ($P < .0001$, $P < .0001$, $P = .0054$), and cellular area ($P < .0001$, $P < .0001$, $P < .0001$) of all lesions (Figure 4; Supplementary Table 1). Combination of 3-BrPA and CB-839 also significantly

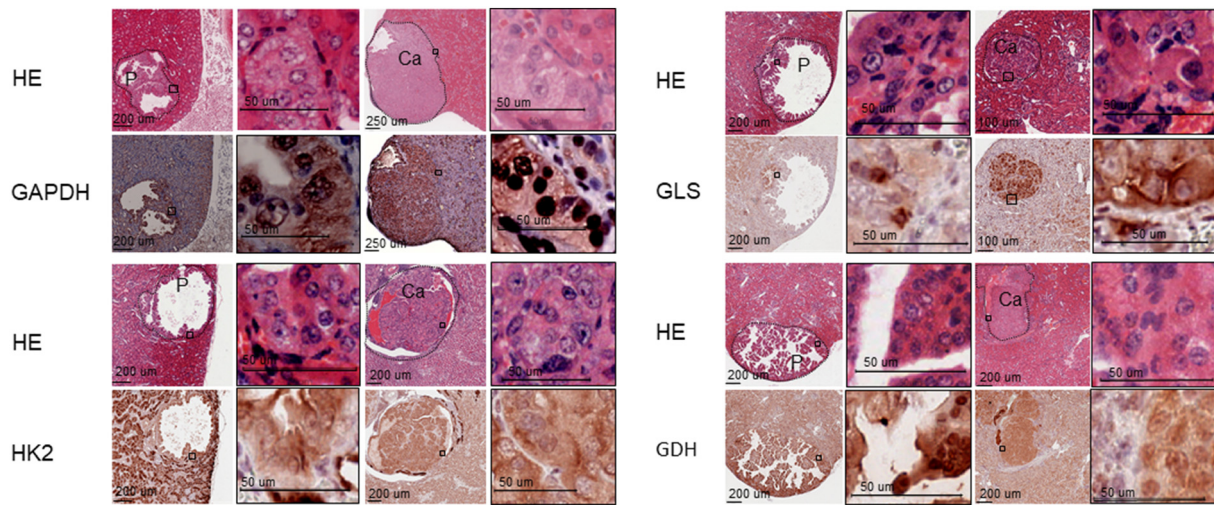


Figure 2. Expression of enzymes crucial for glycolysis and glutaminolysis in renal tumors of $Tsc2^{+/-}$ mice. Kidney sections prepared from 14-month-old $Tsc2^{+/-}$ mice were used for HE and IHC. Protein levels were examined with IHC. Representative stained sections were presented to show expression levels of GAPDH, HK2, GLS, and GDH in renal tumors. Black lines are scale bars.

reduced total number ($P = .0311$), size ($P = .0220$), and cellular area ($P = .0226$) of solid carcinomas (Figure 4; Supplementary Table 2). Similarly, rapamycin alone or rapamycin plus 3-BrPA or rapamycin plus CB-839 again significantly reduced total number ($P < .0001$, $P < .0001$, $P < .0001$), size ($P < .0001$, $P < .0001$, $P < .0001$), and cellular area ($P < .0001$, $P < .0001$, $P < .0001$) of solid carcinomas (Figure 4; Supplementary Table 2). However, 3-BrPA or CB-839 alone did not significantly reduce total number, size, or cellular area of all lesions or solid carcinomas. Notably, rapamycin or rapamycin plus 3-BrPA or rapamycin plus CB-839 reduced tumor burden more

effectively than combination of 3-BrPA and CB-839 in terms of total number, size, and cellular area of all lesions or solid carcinomas alone (Figure 4, Supplementary Tables 1 and 2).

Effect of Treatment on mTOR Signaling and Proliferation in Renal Tumors in $Tsc2^{+/-}$ Mice

We first examined the effect of treatment on mTOR signaling in the kidney tissues by Western blot. We used phosphorylation of S6 ribosomal protein at S235/236 and mTOR at S2448 as readouts for mTORC1 activity and phosphorylation of Akt at S473, Akt at T450,

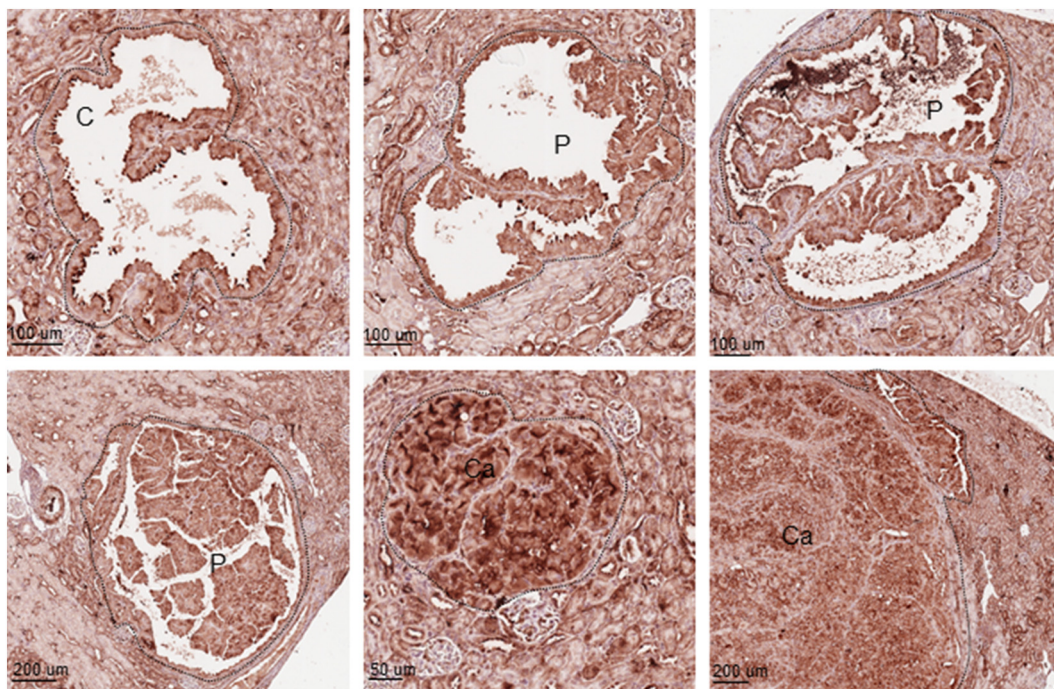


Figure 3. Expression of MCT1 in renal tumors of $Tsc2^{+/-}$ mice. Kidney sections prepared from 14-month-old $Tsc2^{+/-}$ mice were used to detect MCT1 with IHC. Representative stained sections were presented to show MCT1 expression in renal tumors. C, cystic adenomas. Black lines are scale bars.

Table 1. Summary of Animal Treatment

Treatment Group	Number of <i>Tsc2</i> ^{+/-} Mice	Number of Males	Number of Females	Treatment Start Age (Months)	Treatment End Age (Months)	Dosage	Number of Animals Killed Due to Loss of Body Weight Within the First Month of Treatment [†]
Vehicle	17	8	9	12	14	10 μ l/g	0
3-BrPA	19	9	10	12	14	3 mg/kg	3
CB-839	20	9	11	12	14	200 mg/kg	0
Rapamycin	20	8	12	12	14	4 mg/kg	0
3-BrPA+rapamycin	18	8	10	12	14	3 mg/kg+ 4 mg/kg	3
CB-839+rapamycin	20	8	12	12	14	200 mg/kg+ 4 mg/kg	0
3-BrPA+CB-839	18	8	10	12	14	3 mg/kg+ 200 mg/kg	4

* *Tsc2*^{+/-} mice were treated twice daily with vehicle or CB-839 *via* gavage and five times a week with 3-BrPA or rapamycin *via* intraperitoneal injection.

[†] These mice were killed due to significant loss of body weight within the first month of treatment.

mTOR at S2481, and PKC α at T638 for mTORC2 activity. As shown in Figure 5a, rapamycin alone or rapamycin plus 3-BrPA or rapamycin plus CB-839 reduced phosphorylation of S6 ribosomal protein, and rapamycin plus 3-BrPA also reduced phosphorylation of

mTOR at S2448. Combination of 3-BrPA and CB-839 reduced phosphorylation of S6 ribosomal protein although to a lesser degree (Figure 5a). Rapamycin in combination with 3-BrPA or with CB-839 reduced phosphorylation of Akt at S473 and mTOR at S2481, but

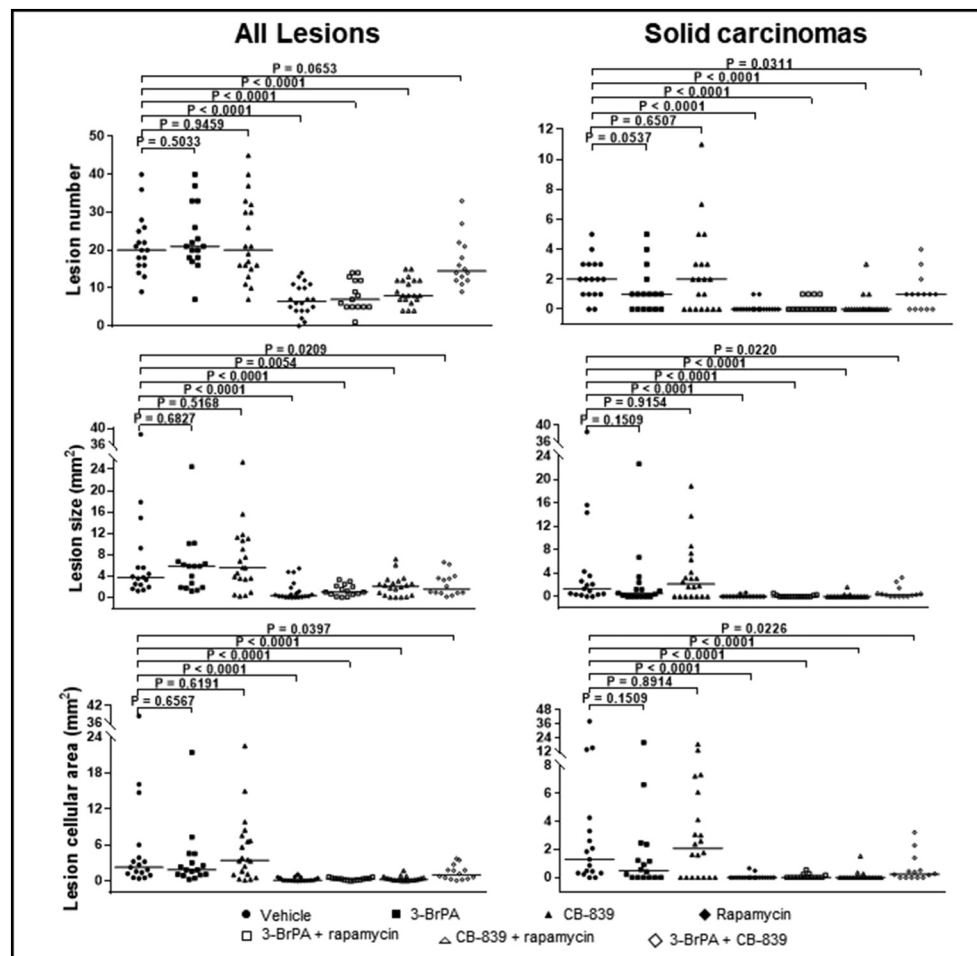


Figure 4. Efficacy of treatment on renal tumors of *Tsc2*^{+/-} mice. *Tsc2*^{+/-} mice were treated from 12 months old for 2 months in 7 groups: vehicle ($n = 17$), 3-BrPA ($n = 19$), CB-839 ($n = 20$), rapamycin ($n = 20$), 3-BrPA+rapamycin ($n = 18$), CB-839 + rapamycin ($n = 20$), and 3-BrPA+CB-839 ($n = 18$). Three mice from the 3-BrPA group, three mice from the 3-BrPA+rapamycin group, and four mice from the 3-BrPA+CB-839 group were euthanized due to significant loss of body weight within the first month of treatment and excluded from further analysis in this study. Dosages are described in methods. After treatment, kidney sections were prepared for histological assessment of treatment efficacy. Left panel: comparison of total number and size (area) as well as cellular area of all lesions (cystic, papillary, and solid). Right panel: comparison of total number and size (area) as well as cellular area of solid carcinomas. Horizontal bars indicate a median. For detailed statistical analysis, see Supplementary Tables 1 and 2.

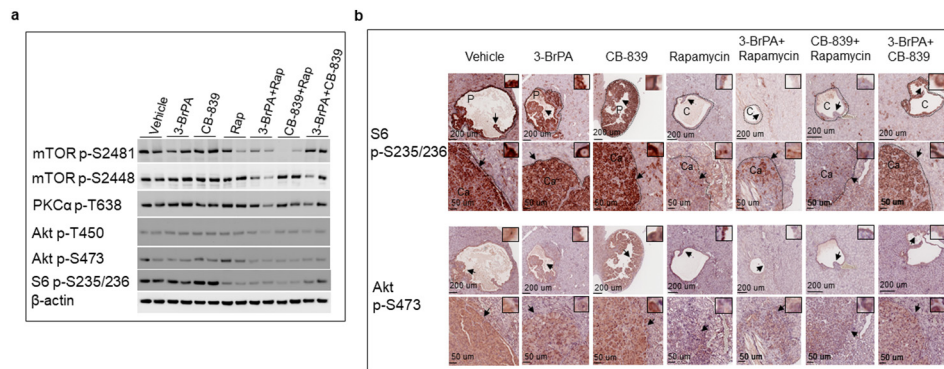


Figure 5. Effect of treatment on mTOR activity in normal tissues and tumors of the kidneys in *Tsc2*^{+/-} mice. (a) Western blot analysis. Proteins were prepared from normal kidney tissues of 14-month-old *Tsc2*^{+/-} mice treated as described above. Beta-actin was used as a loading control. Representative Western blots were presented to show phosphorylation of mTOR at S2448 and S2481, S6 at S235/236, 4E-BP1 at T37/46, Akt at T450 and S473, and PKCα at T638. (b) MS-IHC analysis. Kidney sections were prepared from 14-month-old *Tsc2*^{+/-} mice treated as described above. The same sections were used to stain phosphorylation of S6 at S235/236 and Akt at S473. Representative MS-IHC-stained sections were presented to show phosphorylation of S6 at S235/236 and Akt at S473 in renal tumors. Black lines are scale bars.

rapamycin alone did not (Figure 5a). No consistent changes in phosphorylation of Akt at T450 or PKCα at T638 were observed in the kidney tissues after treatment.

We then assessed effect of treatment on mTOR signaling in renal tumors of *Tsc2*^{+/-} mice by MS-IHC. Similarly, we used phosphorylation of S6 ribosomal protein at S235/236 as a readout for mTORC1 activity and phosphorylation of Akt at S473 as a readout for mTORC2 activity. As shown in Figure 5b, rapamycin alone or rapamycin plus 3-BrPA or rapamycin plus CB-839 consistently reduced phosphorylation of S6 ribosomal protein in cystic/papillary adenomas and solid carcinomas. Combination of 3-BrPA and CB-839 also slightly reduced phosphorylation of S6 ribosomal protein in

cystic/papillary adenomas and solid carcinomas (Figure 5b). Rapamycin plus 3-BrPA or rapamycin plus CB-839 substantially reduced phosphorylation of Akt at S473 in cystic/papillary adenomas and solid carcinomas (Figure 5b). 3-BrPA alone or 3-BrPA plus CB-839 appeared to reduce phosphorylation of Akt at S473 in cystic/papillary adenomas and solid carcinomas although to a lesser degree (Figure 5b). Rapamycin alone reduced phosphorylation of Akt at S473 in solid carcinomas, but a proportion of rapamycin-treated cystic/papillary adenomas showed highly phosphorylated Akt at S473, consistent with previous findings (Figure 5b) [22].

We used Ki67 as a marker to investigate proliferation in renal tumors of *Tsc2*^{+/-} mice by IHC (Figure 6). Fifteen or more renal

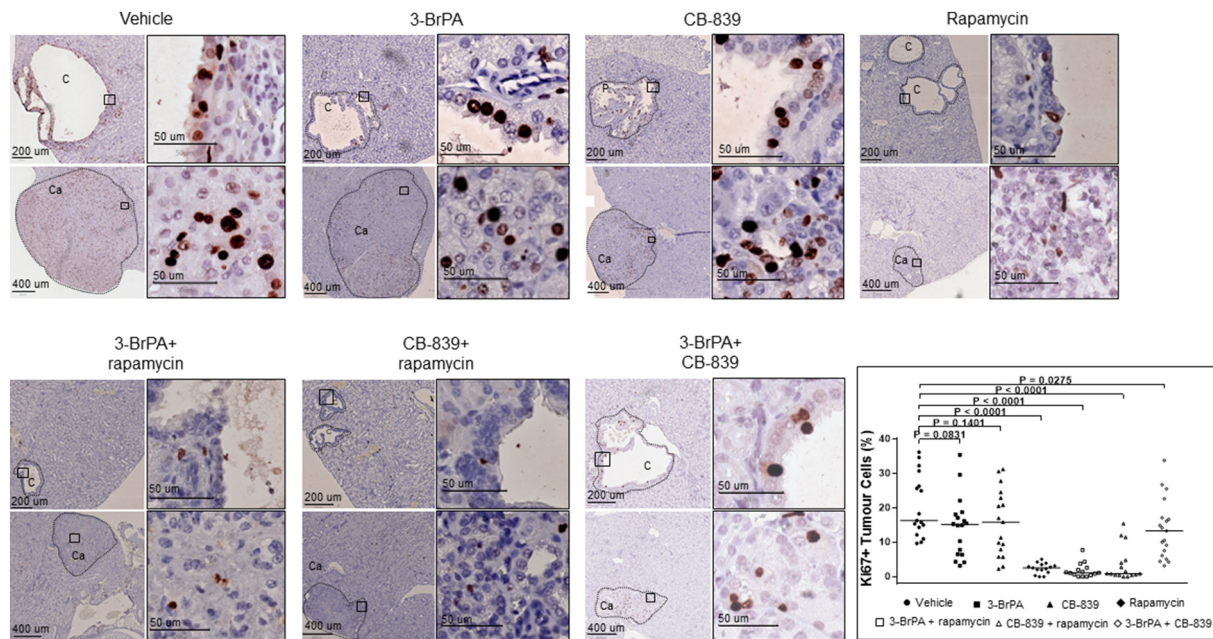


Figure 6. Effect of treatment on proliferation of renal tumor cells in *Tsc2*^{+/-} mice. Kidney sections were prepared from 14-month-old *Tsc2*^{+/-} mice treated as described above and stained with antibody against Ki67 by IHC to assess proliferation of tumor cells. Fifteen or more renal tumors from each treatment group were randomly selected for proliferation analysis. Ki67-positive cells were identified using ImageJ, and percentage of Ki67-positive cells in total tumor cells was used for comparison. Representative sections were presented to show expression of Ki67 in tumor cells. Black lines are scale bars. The right bottom panel shows comparison of percentage of Ki67-positive tumor cells between vehicle and other treatment groups (see Supplementary Tale 3 for detailed statistical analysis.).

tumors from each treatment group were randomly selected for proliferation analysis. Ki67-positive cells were identified using ImageJ, and percentage of Ki67-positive cells in total tumor cells was used for comparison. Rapamycin alone, rapamycin plus 3-BrPA, or rapamycin plus CB-839 substantially reduced the median percentage of Ki67-positive cells from 16.3% to 2.6%, 1.1%, or 0.9%, respectively ($P < .0001$) (Figure 6; Supplementary Table 3). 3-BrPA plus CB-839 also slightly reduced the median percentage of Ki67-positive cells from 16.3% to 13.3% ($P = .0275$) (Figure 6; Supplementary Table 3).

We examined levels of active caspase-3 by IHC to assess apoptosis in renal tumors of *Tsc2*^{+/-} mice. We did not observe any consistent increase in apoptosis in solid carcinomas following treatment (Supplementary Figure 1). In contrast, reduced levels of active caspase-3 were observed in tumors treated with rapamycin alone, rapamycin plus 3-BrPA, or rapamycin plus CB-839. We also noticed that expression of active caspase-3 was very variable in untreated renal tumors and larger carcinomas appeared to have more tumor cells positive for active caspase-3.

Discussion

Upregulated aerobic glycolysis and glutaminolysis are required in rapidly proliferating tumor cells to meet increased energy demands and biosynthetic activity [23]. Inhibition of glycolysis or glutaminolysis has been investigated for treatment of various types of cancer in preclinical studies and clinical trials [24,25]. Dual inhibition of glycolysis with 2-deoxy-glucose and glutaminolysis with aminooxycetate effectively suppressed proliferation of ovarian cancer cells *in vitro* [26]. Nonetheless, tumor therapy through dual inhibition of glycolysis and glutaminolysis has hardly been tested *in vivo*. In this study, we tested the efficacy of dual inhibition of glycolysis and glutaminolysis for therapy of renal lesions in *Tsc2*^{+/-} mice. 3-BrPA is an efficient inhibitor of glycolysis by primarily targeting GAPDH and HK2 [11]. MCT1 is an essential transporter required for 3-BrPA-mediated inhibition of glycolysis [21]. CB-839 is a potent blocker of glutaminolysis by selectively inhibiting GLS [13]. We found that GAPDH, HK2, MCT1, and GLS were all highly expressed in renal carcinomas. We showed that combination of 3-BrPA and CB-839 significantly reduced overall tumor burden when renal carcinomas or all renal lesions (cystic/papillary adenomas and carcinomas) were analyzed in the *Tsc2*^{+/-} mice. These results suggest that the combined treatment may be a better strategy for TSC-associated lesions. However, combination of 3-BrPA and CB-839 was not as efficacious as rapamycin alone or rapamycin in combination with either 3-BrPA or CB-839 for these tumors. Furthermore, significant loss of body weight occurred in some mice treated with 3-BrPA alone, combination of 3-BrPA and rapamycin, or combination of 3-BrPA and CB-839, indicating increased toxicity. Combination of CB-839 and everolimus (a rapamycin analog) has previously showed a greater antitumor activity than everolimus alone in a xenograft mouse model of renal carcinoma and is currently being tested in patients with renal carcinoma [16]. However, we did not find a significant difference in antitumor efficacy between rapamycin alone and rapamycin plus CB-839 in the *Tsc2*^{+/-} mice. Rapamycin/rapalogs alone are therefore likely to be the better option for treatment of TSC-associated renal tumors, while rapalogs combined with CB-839 may improve the treatment for sporadic RCC.

3-BrPA appeared to reduce the burden of renal carcinomas in *Tsc2*^{+/-} mice, but the reduction was not statistically significant. This

finding is different from previous observations demonstrating antitumor efficacy of 3-BrPA for malignancies such as hepatocellular carcinoma, bladder cancer, nasopharyngeal carcinoma, and renal carcinoma *in vitro* and *in vivo* [12,27–29]. Glycolytic inhibition with 2-deoxyglucose also effectively blocked tumor growth in a mouse model transplanted with *Tsc2*-null rat tumor cells [10]. In addition, we did not observe any reduced burden of renal tumors in the *Tsc2*^{+/-} mice treated with CB-839. In contrast, CB-839 was very effective for a variety of cancers in xenograft mouse models [13,15,30], leading to intensive clinical trials currently under way. The poor response of renal lesions to 3-BrPA or CB-839 alone in this study may reflect the specific mechanisms of tumorigenesis in *Tsc2*^{+/-} mice such as the initiating mutations of *Tsc2* and oncogenic mTOR signaling. The differences could also be due to xenograft mouse models used in previous studies that were distinct from genetically altered mice used in this study.

CB-839 has recently been granted Fast Track Designation by the US Food and Drug Administration for combination with cabozantinib to treat patients with metastatic renal cell carcinoma. Cabozantinib is an inhibitor of multiple tyrosine kinases including vascular endothelial growth factor receptors (VEGFRs) [31] and has demonstrated potent antitumor efficacy in a xenograft model of colorectal cancer through inhibition of angiogenesis and Akt activity [32]. A recent clinical trial of cabozantinib has shown significantly improved overall and progression-free survival of patients with advanced renal cell carcinoma [33]. Expression of VEGFR1 is increased and Akt is activated in TSC-associated renal tumors [19,34]. Further investigations may, therefore, be worthwhile to compare CB-839 combined with cabozantinib with rapamycin or its analogs for TSC-associated renal lesions in *Tsc2*^{+/-} mice.

We examined the effect of treatment on mTOR signaling in normal tissues and tumors from the kidneys of *Tsc2*^{+/-} mice. Rapamycin alone or rapamycin in combination with either 3-BrPA or CB-839 potently inhibited mTORC1, while combination of 3-BrPA and CB-839 only slightly decreased mTORC1 activity in both normal and tumor tissues. Such mTORC1 inhibition was associated with reduced proliferation of tumor cells, possibly accounting for antitumor activity of these treatments, with rapamycin alone or rapamycin in combination with either 3-BrPA or CB-839 being significantly more effective for these tumors in *Tsc2*^{+/-} mice. Notably, rapamycin alone or rapamycin in combination with either 3-BrPA or CB-839 was much more efficient in reducing lesion number than combination of 3-BrPA and CB-839, consistent with a role of mTORC1 inhibition in prevention of TSC-associated tumor formation [19]. CB-839 was reported to substantially decrease mTORC1 activity in CB-839-sensitive tumor cells of renal carcinomas [16]. However, we did not observe any inhibitory activity of CB-839 on mTORC1 in TSC-associated renal tumors, and this could partly explain the lack of response of these tumors to CB-839 alone. Combination of rapamycin with 3-BrPA or with CB-839 strongly inhibited mTORC2 in all renal lesions including cystic/papillary adenomas and solid carcinomas, but rapamycin alone in contrast increased signaling of mTORC2 in a proportion of cystic/papillary adenomas. 3-BrPA alone or in combination with CB-839 also inhibited mTORC2 in all lesions although to a lesser degree. Feedback increase of mTORC2 activity after rapamycin treatment is believed to be one of the reasons for limited efficacy [35]. However, inhibition of mTORC2 may promote or suppress death of tumor cells depending on cellular contexts [36,37]. In addition, no increased apoptosis was observed in renal tumors treated with any single or combined compounds in this study. It remains to be further

examined whether inhibition of mTORC2 contributes to antitumor efficacy in TSC-associated renal lesions.

We conclude that combination of 3-BrPA and CB-839 may not offer a better therapeutic strategy than rapamycin for TSC-associated tumors, although the combination therapy significantly reduced overall size of all renal lesions.

Supplementary data to this article can be found online at <https://doi.org/10.1016/j.neo.2018.12.003>.

Conflict of Interest Statement

The authors declare no conflict of interest.

Acknowledgements

We would like to thank Dr. David Kwiatkowski for providing the *Tsc2*^{+/-} mouse model. CB-839 was kindly provided by Calithera Biosciences, Inc., South San Francisco, CA. This project was supported by the Wales Gene Park, UK, and the Tuberous Sclerosis Association, UK.

References

- [1] Consortium ECTS (1993). Identification and characterization of the tuberous sclerosis gene on chromosome 16. *Cell* **75**(7), 1305–1315.
- [2] Huang J and Manning BD (2009). A complex interplay between Akt, TSC2 and the two mTOR complexes. *Biochem Soc Trans* **37**(Pt 1), 217–222.
- [3] Henske EP, Wessner LL, Golden J, Scheithauer BW, Vortmeyer AO, Zhuang Z, Klein-Szanto AJ, Kwiatkowski DJ, and Yeung RS (1997). Loss of tuberlin in both subependymal giant cell astrocytomas and angiomyolipomas supports a two-hit model for the pathogenesis of tuberous sclerosis tumors. *Am J Pathol* **151**(6), 1639–1647.
- [4] Tyburczy ME, Jozwiak S, Malinowska IA, Chekaluk Y, Pugh TJ, Wu CL, Nussbaum RL, Seepo S, Dzik T, and Kotulska K, et al (2015). A shower of second hit events as the cause of multifocal renal cell carcinoma in tuberous sclerosis complex. *Hum Mol Genet* **24**(7), 1836–1842.
- [5] Bissler JJ, McCormack FX, Young LR, Elwing JM, Chuck G, Leonard JM, Schmithorst VJ, Laor T, Brody AS, and Bean J, et al (2008). Sirolimus for angiomyolipoma in tuberous sclerosis complex or lymphangiomyomatosis. *N Engl J Med* **358**(2), 140–151.
- [6] Davies DM, de Vries PJ, Johnson SR, McCartney DL, Cox JA, Serra AL, Watson PC, Howe CJ, Doyle T, and Pointon K, et al (2011). Sirolimus therapy in tuberous sclerosis or sporadic lymphangiomyomatosis. *Clin Cancer Res* **17**(12), 4071–4081.
- [7] Bissler JJ, Kingswood JC, Radzikowska E, Zonnenberg BA, Frost M, Belousova E, Sauter M, Nonomura N, Brakemeier S, and de Vries PJ, et al (2013). Everolimus for angiomyolipoma associated with tuberous sclerosis complex or sporadic lymphangiomyomatosis (EXIST-2): a multicentre, randomised, double-blind, placebo-controlled trial. *Lancet* **381**(9869), 817–824.
- [8] Choo AY, Kim SG, Vander Heiden MG, Mahoney SJ, Vu H, Yoon SO, Cantley LC, and Blenis J (2010). Glucose addiction of TSC null cells is caused by failed mTORC1-dependent balancing of metabolic demand with supply. *Mol Cell* **38**(4), 487–499.
- [9] Csibi A, Fendt SM, Li C, Poulgiannis G, Choo AY, Chapski DJ, Jeong SM, Dempsey JM, Parkhitko A, and Morrison T, et al (2013). The mTORC1 pathway stimulates glutamine metabolism and cell proliferation by repressing SIRT4. *Cell* **153**(4), 840–854.
- [10] Jiang X, Kenerson HL, and Yeung RS (2011). Glucose deprivation in tuberous sclerosis complex-related tumors. *Cell Biosci* **1**, 1–15.
- [11] Tang Z, Yuan S, Hu Y, Zhang H, Wu W, Zeng Z, Yang J, Yun J, Xu R, and Huang P (2012). Over-expression of GAPDH in human colorectal carcinoma as a preferred target of 3-bromopyruvate propyl ester. *J Bioenerg Biomembr* **44**(1), 117–125.
- [12] Ko YH, Verhoeven HA, Lee MJ, Corbin DJ, Vogl TJ, and Pedersen PL (2012). A translational study "case report" on the small molecule "energy blocker" 3-bromopyruvate (3BP) as a potent anticancer agent: from bench side to bedside. *J Bioenerg Biomembr* **44**(1), 163–170.
- [13] Gross MI, Demo SD, Dennison JB, Chen L, Chernov-Rogan T, Goyal B, Janes JR, Laidig GJ, Lewis ER, and Li J, et al (2014). Antitumor activity of the glutaminase inhibitor CB-839 in triple-negative breast cancer. *Mol Cancer Ther* **13**(4), 890–901.
- [14] Matre P, Shariati M, Velez J, Qi Y, Konoplev S, Su X, DiNardo CD, Daver N, Majeti R, and Andreeff M, et al (2014). Efficacy of novel glutaminase inhibitor CB-839 in acute myeloid leukemia. *Blood* **124**(21), 3763.
- [15] Xiang Y, Stine ZE, Xia J, Lu Y, O'Connor RS, Altman BJ, Hsieh AL, Gouw AM, Thomas AG, and Gao P, et al (2015). Targeted inhibition of tumor-specific glutaminase diminishes cell-autonomous tumorigenesis. *J Clin Invest* **125**(6), 2293–2306.
- [16] Emberley E, Bennett M, Chen J, Gross M, Huang C, Li A, MacKinnon A, Pan A, Rodriguez M, and Steggerda S, et al (2017). CB-839, a selective glutaminase inhibitor, has anti-tumor activity in renal cell carcinoma and synergizes with cabozantinib and everolimus. *Keystone Symposia*; 2017.
- [17] Onda H, Lueck A, Marks PW, Warren HB, and Kwiatkowski DJ (1999). *Tsc2* (+/-) mice develop tumors in multiple sites that express gelsolin and are influenced by genetic background. *J Clin Invest* **104**(6), 687–695.
- [18] Kalogerou M, Zhang Y, Yang J, Garrahan N, Paisey S, Tokarczuk P, Stewart A, Gallacher J, Sampson JR, and Shen MH (2012). T2 weighted MRI for assessing renal lesions in transgenic mouse models of tuberous sclerosis. *Eur J Radiol* **81**(9), 2069–2074.
- [19] Yang J, Kalogerou M, Samsel PA, Zhang Y, Griffiths DF, Gallacher J, Sampson JR, and Shen MH (2015). Renal tumours in a *Tsc2*(+/-) mouse model do not show feedback inhibition of Akt and are effectively prevented by rapamycin. *Oncogene* **34**(7), 922–931.
- [20] Kim M, Soontornniyomkij V, Ji B, and Zhou X (2012). System-wide immunohistochemical analysis of protein co-localization. *PLoS One* **7**(2):e32043.
- [21] Birsoy K, Wang T, Possemato R, Yilmaz OH, Koch CE, Chen WW, Hutchins AW, Gultekin Y, Peterson TR, and Carette J, et al (2015). Renal tumours in a *Tsc2*(+/-) mouse model do not show feedback inhibition of Akt and are effectively prevented by rapamycin. *Oncogene* **34**(7), 922–931.
- [22] Narov K, Yang J, Samsel PA, Jones A, Sampson JR, and Shen M (2017). The dual PI3K/mTOR inhibitor GSK2126458 is effective for treating solid renal tumours in *Tsc2*+/- mice through suppression of cell proliferation and induction of apoptosis. *Oncotarget* **8**(35), 58504–58512.
- [23] Cairns RA, Harris IS, and Mak TW (2011). Regulation of cancer cell metabolism. *Nat Rev Cancer* **11**(2), 85–95.
- [24] Martinez-Outschoorn UE, Peiris-Pages M, Pestell RG, Sotgia F, and Lisanti MP (2017). Cancer metabolism: a therapeutic perspective. *Nat Rev Clin Oncol* **14**(1), 11–31.
- [25] Akins NS, Nielson TC, and Le HV (2018). Inhibition of glycolysis and glutaminolysis: an emerging drug discovery approach to combat cancer. *Curr Top Med Chem* **18**(6), 494–504.
- [26] Sun L, Yin Y, Clark LH, Sun W, Sullivan SA, Tran AQ, Han J, Zhang L, Guo H, and Madugu E, et al (2017). Dual inhibition of glycolysis and glutaminolysis as a therapeutic strategy in the treatment of ovarian cancer. *Oncotarget* **8**(38), 63551–63561.
- [27] Konstantakou EG, Voutsinas GE, Velentzas AD, Basogianni AS, Paronis E, Balafas E, Kostomitsopoulos N, Syrigos KN, Anastasiadou E, and Stravopodis DJ (2015). 3-BrPA eliminates human bladder cancer cells with highly oncogenic signatures via engagement of specific death programs and perturbation of multiple signaling and metabolic determinants. *Mol Cancer* **14**, 1–26.
- [28] Zou X, Zhang M, Sun Y, Zhao S, Wei Y, Zhang X, Jiang C, and Liu H (2015). Inhibitory effects of 3-bromopyruvate in human nasopharyngeal carcinoma cells. *Oncol Rep* **34**(4), 1895–1904.
- [29] Nilsson H, Lindgren D, Mandahl Forsberg A, Mulder H, Axelson H, and Johansson ME (2015). Primary clear cell renal carcinoma cells display minimal mitochondrial respiratory capacity resulting in pronounced sensitivity to glycolytic inhibition by 3-bromopyruvate. *Cell Death Dis* **6**, e1585.
- [30] Abu About O, Habib SL, Trott J, Stewart B, Liang S, Chaudhari AJ, Sutcliffe J, and Weiss RH (2017). Glutamine addiction in kidney cancer suppresses oxidative stress and can be exploited for real-time imaging. *Cancer Res* **77**(23), 6746–6758.
- [31] Markowitz JN and Fancher KM (2018). Cabozantinib: a multitargeted oral tyrosine kinase inhibitor. *Pharmacotherapy* **38**(3), 357–369.
- [32] Song EK, Tai WM, Messersmith WA, Bagby S, Purkey A, Quackenbush KS, Pitts TM, Wang G, Blatchford P, and Yahn R, et al (2015). Potent antitumor activity of cabozantinib, a c-MET and VEGFR2 inhibitor, in a colorectal cancer patient-derived tumor explant model. *Int J Cancer* **136**(8), 1967–1975.
- [33] Osanto S and van der Hulle T (2018). Cabozantinib in the treatment of advanced renal cell carcinoma in adults following prior vascular endothelial growth factor targeted therapy: clinical trial evidence and experience. *Ther Adv Urol* **10**(3), 109–123.

- [34] Yang J, Samsel PA, Narov K, Jones A, Gallacher D, Gallacher J, Sampson JR, and Shen MH (2017). Combination of everolimus with sorafenib for solid renal tumors in *Tsc2(+/-)* mice is superior to everolimus alone. *Neoplasia* **19**(2), 112–120.
- [35] Wan X, Harkavy B, Shen N, Grohar P, and Helman LJ (2007). Rapamycin induces feedback activation of Akt signaling through an IGF-1R–dependent mechanism. *Oncogene* **26**(13), 1932–1940.
- [36] Goncharova EA, Goncharov DA, Li H, Pimtong W, Lu S, Khavin I, and Krymskaya VP (2011). xmTORC2 is required for proliferation and survival of *TSC2*-null cells. *Mol Cell Biol* **31**(12), 2484–2498.
- [37] Khan MW, Biswas D, Ghosh M, Mandloi S, Chakrabarti S, and Chakrabarti P (2015). mTORC2 controls cancer cell survival by modulating gluconeogenesis. *Cell Death Discov* **11**5016.